LETTER TO THE EDITOR

The melting temperature of a two-dimensional electron solid on helium in a magnetic field

A O Stone, M J Lea, P Fozooni and J Frost

Department of Physics, Royal Holloway and Bedford New College, University of
London, Egham, Surrey TW20 0EX, UK

Abstract. The melting temperature of a 2D electron solid, density 8×10^{12} m^{-2}, on liquid
helium has been found to be almost independent of magnetic field from 0.5 to 7 T.

The melting of a two-dimensional electron crystal has been the subject of much interest
in the last decade. For the classical solid first observed by Grimes and Adams [1] in
electrons above liquid helium, the transition is best described by the Kosterlitz–Thouless
model. The melting temperature of the classical crystal $T_{mc} = (\pi n)^{1/2} e^2 / 4\pi \bar{\varepsilon}\varepsilon_0 k_B \Gamma_m$,
where n is the electron density, $\bar{\varepsilon} = (\varepsilon_v + \varepsilon_l)/2$ is the average of the vapour and liquid
dielectric constants, k_B is the Boltzmann constant and Γ_m is the ratio of the mean potential
energy to the mean kinetic energy and has a value 127 ± 3 [2]. Only small [3] or no
[4] quantum corrections to the melting temperature have been observed for electron
densities up to 3×10^{14} m^{-2}. At much higher densities, zero-point motion will reduce
the melting temperature T_m below T_{mc} [5, 6, 7, 8], until above a critical density the
electrons remain fluid to the lowest temperatures. However, in this quantum region a
magnetic field B should suppress the zero-point motion and induce 2D Wigner crys-
tallisation as has recently been reported in GaAs/GaAlAs heterojunctions [9].

In this Letter we present measurements of the effect of a magnetic field up to 7 T on
the melting temperature of a classical 2D electron gas (2DEG) above the surface of liquid
^{4}He. We detect the crystallisation in a cell designed to measure the magnetoresistance
using the Sommer–Tanner technique [10]. The rectangular cell consisted of parallel
upper and lower plates 1.96 ± 0.03 mm apart surrounded by a vertical guard-ring
(dimensions 17.5 mm $\times$ 7.0 mm). Liquid helium was condensed between the plates to
a depth $d = 0.45$ mm at 0.9 K. The helium surface was charged using a glow discharge,
and was parallel to the lower plate to better than 2 mrad. The lower plate was an array
of three co-planar rectangular electrodes (see figure 1(a)), at a common DC potential.
Electrode A was driven with an AC voltage at frequencies $13 \leqslant f = \omega/2\pi \leqslant 72$ kHz which
capacitatively coupled to the electrons. The in-phase and quadrature components of the
current I (0°) and I(90°) that flowed to electrode D were phase referenced to the drive
voltage and measured with a lock-in amplifier. Electrode E was kept at AC ground.

The temperature was measured using carbon resistance thermometry calibrated
against a CMN thermometer and an SRM 767 superconducting fixed point thermometer.
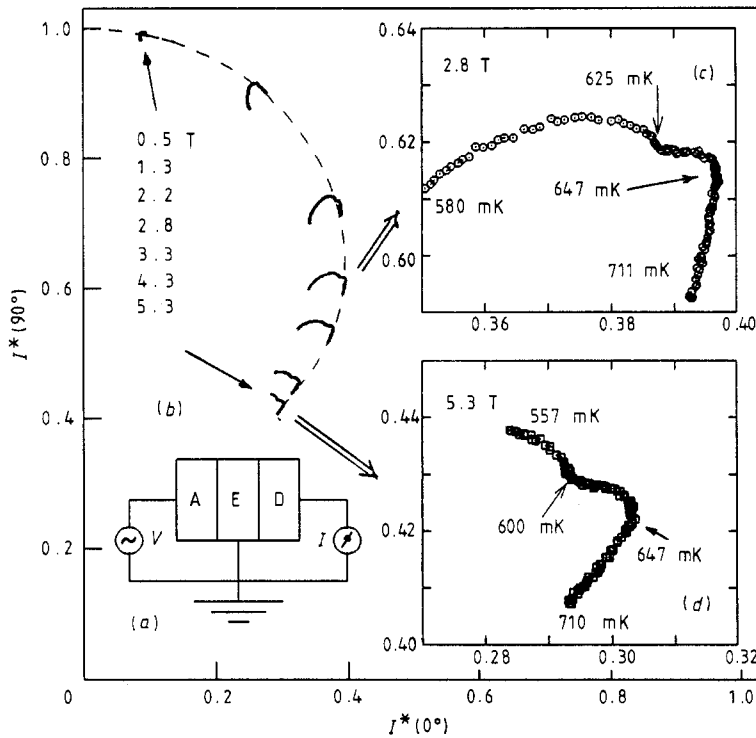
Figure 1. (*a*) The electrode arrangement for measuring the field dependent crystallisation of a 2D electron gas. Electrode A was excited with an AC voltage. The in-phase, $I(0°)$, and quadrature, $I(90°)$, components of current to electrode D were measured. (*b*) The current I^* plotted on an Argand diagram, normalised to the magnitude of the current in zero field. The broken curve shows the locus of I^* at 32.13 kHz as the field was increased to 5.3 T. Data at constant fields from 0.5 to 5.3 T are shown from 710 to 550 mK. (*c*) Expanded plot of the data at 2.8 T from 580 to 711 mK. The melting temperature is taken as the point at 647 ± 2 mK where the initial change in the locus of I^* occurs. A second feature at 625 mK is marked. (*d*) Expanded plot of the data at 5.3 T from 557 to 710 mK. The melting temperature is taken as the point at 647 ± 3 mK where the initial change in the locus of I^* occurs. A second feature at 600 mK is marked.

We estimate an uncertainty in T of 1 mK in the temperature and field range of our experiment (550–700 mK and 0–7 T respectively).

In zero magnetic field below 1 K, the resistance of the electron sheet was small and the current I was close to 90° to the applied voltage. The application of a field changed the magnitude and phase of the current. For a fully screened electron gas, an AC driving voltage excites a heavily damped wave [11] with a wavevector, k, parallel to the AC electric field and of magnitude given by

$$|k| = (1 - j)/\delta \qquad \delta = (2\sigma_{xx}/\omega C')^{1/2} \tag{1}$$

where C' is the capacitance per unit area between the electrons and the electrodes and σ_{xx} is the magnetoconductivity for $\omega\tau \ll 1$ where τ is a scattering time. The components of k parallel and perpendicular to the current flow (and hence the edges of the electron sheet) are
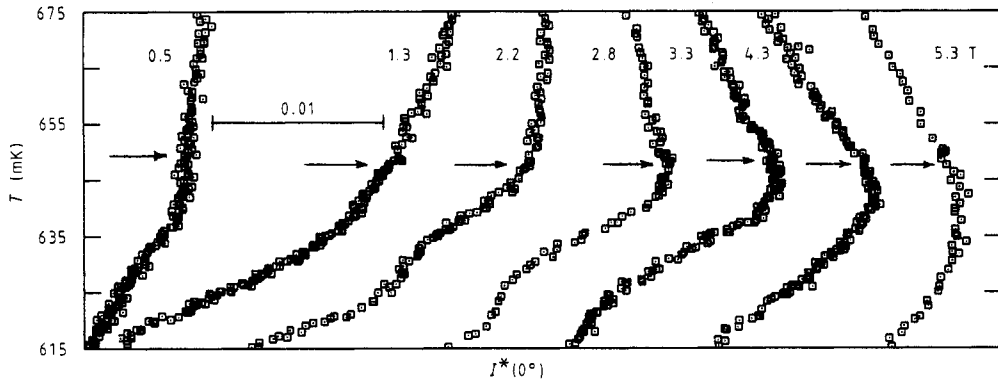
Figure 2. The temperature dependence of the current component $I^*(0°)$ at fields from 0.5 to 5.3 T as shown in figure 1. The temperature T_m at which a change in the locus of I^* occurs is marked. The magnitude of a change in $I^*(0°)$ of 0.01 is shown.

$$k_\parallel = (1 - \text{j})/\delta_\parallel \qquad \delta_\parallel = (2/\omega C' \rho_{xx})^{1/2}$$
$$k_\parallel = (1 - \text{j})/\delta_\perp \qquad \delta_\perp = (\rho_{xx}/\rho_{xy})\delta_\parallel \tag{2}$$

where ρ_{xx} and ρ_{xy} are components of the magnetoresistivity tensor. For low temperatures (and hence high electron mobility μ) $\delta_\parallel$ is much greater than the sample size, and the measured current I to electrode D depends only on $\delta_\perp$. As $\delta_\perp$ varies, due to a change in field, temperature or frequency, $I(0°)$ and $I(90°)$ should follow a distinctive locus on an Argand diagram determined by the geometry of the electron sheet. This is confirmed experimentally by the broken curve in figure 1(b) which shows the variation of the normalised current I^* in the electron fluid phase at 700 mK as the field was increased. The current has been normalised to its value in zero field, where the phase was 90°. Any variation in resistivity alone should change I^* along this locus.

As the temperature was reduced below 700 mK in constant field, $\delta_\perp$ increased and the measured I^* moved round the locus on the Argand diagram, as shown in figure 1(b) for magnetic fields of 0.5, 1.3, 2.2, 2.8, 3.3, 4.3 and 5.3 T using a measurement frequency of 32 kHz. However, as the electrons were cooled into the solid phase, a sharp change in the locus of I^* was observed. We interpret this as the onset of electron crystallisation. Expanded plots of the typical signatures of the phase transition are shown in figures 1(c) and 1(d). We use the position of the first departure from the fluid locus of I^* to define the transition temperature as marked. The temperature dependence of $I^*(0°)$ for these fields is shown in figure 2. In the fluid phase the current is temperature dependent as ρ_{xx} changes, and the gradient depends on the position on the Argand diagram. In each case the transition at T_m as determined from the Argand diagram is shown. The origin of the signature of the crystallisation is as follows. The wave vector k of the propagating wave will be modified in the crystal, which can support a shear wave, with velocity c_t and can be derived from the dynamical matrix (Shikin and Williams [12]) as

$$|k| = [(1 - \text{j})/\delta](1 + c_t^2 \tau/\omega\delta^2 - \text{j}\,\omega\tau/2) \tag{3}$$

for $\omega\tau \ll 1$ (but finite), $\mu B \gg 1$. At the phase transition, c_t increases rapidly as the shear mode starts to propagate [13]. Also, at low frequencies, the electron effective mass m^* is enhanced by electron–ripplon coupling in the solid phase and by the formation of
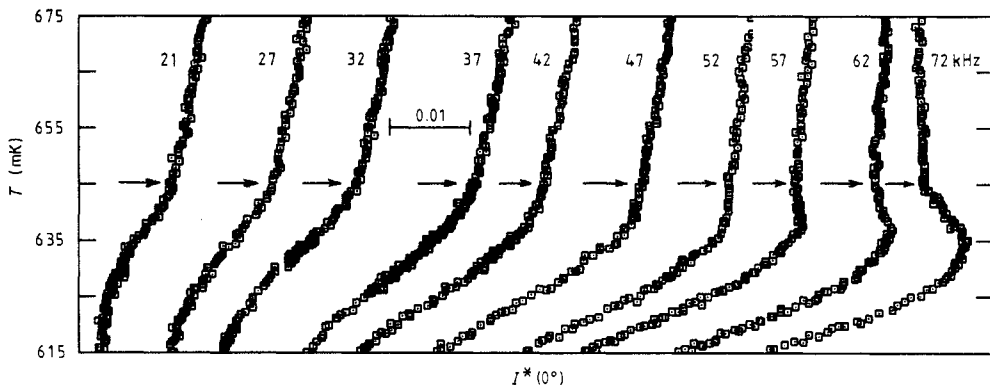
Figure 3. The measured currents $I^*(0°)$ versus temperature at 1.1 T at frequencies from 21 to 72 kHz. The temperature T_m at which a change in the locus of I^* occurs is marked. The magnitude of a change in $I^*(0°)$ of 0.01 is shown.

ripplon standing waves [2, 14]. Since $\tau = m^*\mu/e$, $\omega\tau$ will increase rapidly just below T_m where m^* is much more temperature dependent than μ. We have estimated the effects of these changes on our measurements and find that the dominant factor close to the transition is the increase in m^* and hence $\omega\tau$. The real and imaginary components of the complex wave vector k, equation (3), are no longer equal and the measured current deviates sharply from the fluid locus at T_m.

Using this criterion we have measured T_m for three crystals in magnetic fields from 0.5 to 7 T. In each case the maximum electron concentration as calculated from the charging potentials was $n = (8.1 \pm 0.5) \times 10^{12}\,\text{m}^{-2}$, which would give a zero-field melting temperature of 640 ± 20 mK using $\Gamma_m = 127 \pm 3$ [2]. The actual density varied slightly between runs but was constant throughout each set of measurements, as shown by carefully checking the reproducibility of the data at each frequency and field.

At each magnetic field, measurements were made at different frequencies as shown in figure 3 at a field of 1.1 T. At low frequencies, $I^*(0)$ decreases at T_m as shown. As the frequency increases, a temperature dependent peak occurs which can mask the transition as seen in this component of I^*. It was essential to inspect both components of I^* to locate the transition. No frequency dependence of T_m was observed, within the error bars. At much higher frequencies, $f > 1$ MHz, Guo *et al* [15] showed that the effective melting temperature increased slightly with frequency, as expected for a Kosterlitz–Thouless transition. However, below 100 kHz, this effect should be small. The value of $\delta_\perp$ was typically 2–3 mm, so the experiments sampled the whole electron sheet and the crystallisation would presumably start at the region of highest density in the centre. The measured T_m was independent of the excitation voltage up to 40 mV amplitude and no heating or non-linear effects were seen at the voltages used. No thermal hysteresis was observed on warming or cooling through the transition. The melting temperature T_m for the three crystals is shown in figure 4(*a*), (*b*) and (*c*), and was found to be almost independent of field within the error bars, though there is some evidence that T_m decreases slightly as the field increases. We were unable to detect the transition in zero field at the frequencies used.

In the classical, low density limit, a magnetic field should have no effect on the thermodynamic properties of a 2D electron crystal. At finite densities, the field dependence of T_m should give a good measure of the quantum corrections to the classical
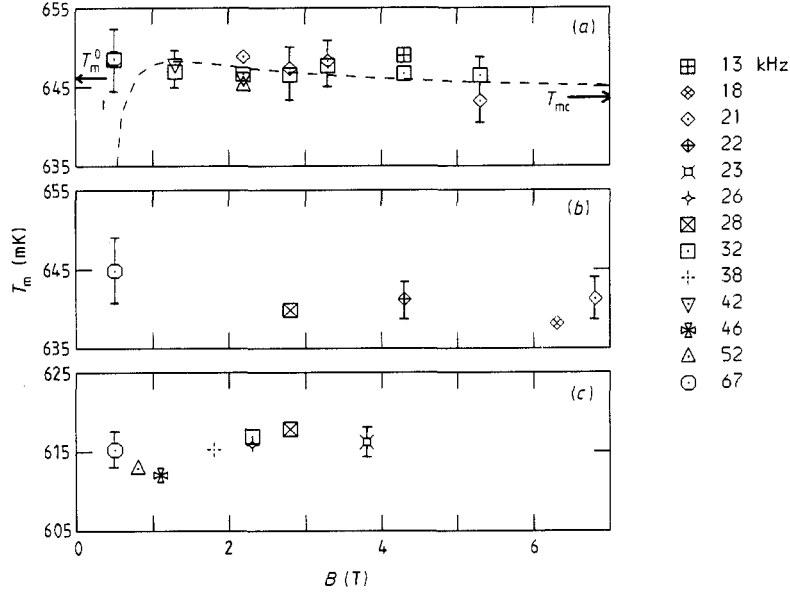
Figure 4. The field dependence of T_m for three separate experimental runs ((a), (b) and (c)). Measurements were made at fields from 0.5 to 7 T and at frequencies from 13 to 67 kHz. The broken curve shows the theoretical calculation of T_m from equation (6) for $T_{mc} = 643.5$ mK as marked. The calculations by Chang and Maki [8] give $T_m^0 = 646$ mK in zero field, as marked, for $T_{mc} = 643.5$ mK.

melting temperature T_{mc}. In zero field, Mehrotra *et al* [3] found a reduction in the melting temperature T_m^0 given by

$$T_m^0 = T_{mc}/(1 + An^{1/2}) \qquad (4)$$

where $A = 9 \times 10^{-9}$ m. This gives $\Delta T_m^0 = T_m^0 - T_{mc} = -16$ mK at $n = 8.1 \times 10^{12}$ m^{-2}. Kajita [4] measured the melting temperature for 2D electrons on solid neon for $n \leqslant 3 \times 10^{14}$ m^{-2} and found no significant quantum effects, though an extrapolation of equation (4) lies within the error bars on his data. Kono [16] and Deville [2] have also measured T_m^0 for electrons on helium for densities up to 12×10^{12} m^{-2} and their results agree with the purely classical result within their error bars.

The field dependence of T_m has been calculated by Saitoh [7] from the mag-netoplasmon modes using a Lindemann criterion. These calculations predict substantial quantum effects at relatively low densities, giving $\Delta T_m^0 = -90$ mK at $n = 8.1 \times 10^{12}$ m^{-2}, with T_m increasing in low fields at $\simeq 15$ mK T^{-1}, a much bigger change than found experimentally. The shear modulus $\mu(B, T)$ has been calculated by Fisher [6] for a high density crystal in the high field classical limit as

$$\mu(B, T)/\mu_0 = 1 - \Gamma^{-1}(26.5 - 0.54\,\nu\Gamma + 0.078\,\nu^2\Gamma^2) \qquad (5)$$

where μ_0 is the low temperature shear modulus of the classical crystal, $\nu = nh/eB$ is the Landau level filling factor in the fluid phase, and $\Gamma = \Gamma_m T_{mc}/T$. (Note that we have obtained equation (5) from equations (2.19) and (4.1) in the paper by Fisher; two of the

coefficients differ by factors of 10 from his equation (4.2).) Applying the Kosterlitz–Thouless melting criterion $\mu = 4\,\pi k T_{\rm m}/a^2$, where a is the lattice parameter, gives

$$T_{\rm m} = T_{\rm mc}(1 + 0.54\,\nu - 9.91\,\nu^2).\tag{6}$$

For our experiments $\nu = 0.0335/B > 0.005$ where B is in tesla. The field dependence of the melting temperature for $T_{\rm mc} = 643.5$ mK given by equation (6) is shown in figure 4(a). Note that $T_{\rm m}$ should be slightly greater than $T_{\rm mc}$ above 1 T, but decreases below $T_{\rm mc}$ at lower fields. This theoretical expression is only valid in the high field limit and diverges for $\nu\Gamma > 1$. It also assumes that the cyclotron frequency is much greater than the lattice frequencies, which is not the case in our experiments. At high fields, the predicted change in $T_{\rm m}$ is small and within the experimental error bars. Chang and Maki [8] have calculated the anharmonic and quantum corrections to μ in zero field, and give the melting temperature as

$$T_{\rm m}^0 \approx T_{\rm mc}(1 + 17.98\,r_{\rm s}^{-1} - 12647\,r_{\rm s}^{-2})\tag{7}$$

where $r_{\rm s} = (\pi n a_{\rm B}^2)^{-1/2}$ is the ratio of the Wigner–Seitz radius to the Bohr radius $a_{\rm B}$, and has the value of 3700 in our experiments. Note that $T_{\rm m}^0 > T_{\rm mc}$ for $r_{\rm s} > 700$ in this expression. For $T_{\rm mc} = 643.5$ mK (the value in high field), $T_{\rm m} = 646$ mK in zero field. This change is in reasonable agreement with an extrapolation of Fisher's calculation and is marked on figure 4(a). We conclude that quantum effects on the melting of 2D electrons are small at the densities studied here. Our results are consistent, within the error bars, with the theoretical calculations of Fisher [6] and Chang and Maki [8]. Experiments at higher densities and higher fields would be most interesting. Further theoretical work is also required.

Below $T_{\rm m}$ another feature, represented by a sharp change in the Argand diagram locus, was observed in these experiments as indicated in the expanded Argand diagrams in figures 1(c) and 1(d). The temperature T_1 at which this feature occurred decreased linearly with field at 9 mK T^{-1} and was independent of frequency (though it was more pronounced at higher frequencies). The origin of this feature is not known, though it could be a field dependent loss peak or even a second phase transition.

References

[1] Grimes C C and Adams G 1979 *Phys. Rev. Lett.* **42** 795
[2] Deville G 1988 *J. Low Temp. Phys.* **72** 135
[3] Mehrotra R, Guenin B M and Dahm A J 1982 *Phys. Rev. Lett.* **48** 641
[4] Kajita K 1985 *J. Phys. Soc. Japan.* **54** 4092
[5] Peeters F M 1984 *Phys. Rev.* B **30** 159
    Fukuyama H, Platzman P M and Anderson P W 1979 *Phys. Rev.* B **19** 5211
    Fukuyama H and Yoshioka D 1980 *J. Phys. Soc. Japan* **48** 1853
    Lozovik Yu E, Fartzdinov V M and Abdullaev B 1985 *J. Phys. C: Solid State Phys.* **18** L807
[6] Fisher D S 1982 *Phys. Rev.* B **26** 5009
[7] Saitoh M 1988 *Surf. Sci.* **196** 8
[8] Chang M and Maki K 1983 *Phys. Rev.* B **27** 1646
[9] Andrei E Y, Deville G, Glattli D C, Williams F I B, Paris E and Etienne B 1988 *Phys. Rev. Lett.* **60** 2765

Glattli D C, Deville G, Dubureq V, Williams F I B, Paris E, Etienne B and Andrei E Y 1990 *Surf. Sci.* at press

[10] Sommer W T and Tanner D J 1971 *Phys. Rev. Lett.* **27** 1345
Stone A O, Fozooni P, Lea M J and Abdul-Gader M 1989 *J. Phys.: Condens. Matter* **1** 2743

[11] Lea M J, Stone A O and Fozooni P 1988 *Europhys. Lett.* **7** 641

[12] Shikin V B and Williams F I B 1981 *J. Low Temp. Phys.* **43** 1

[13] Gallet F, Deville G, Valdès A and Williams F I B 1982 *Phys. Rev. Lett.* **49** 212
Deville G, Valdès A, Andrei E Y and Williams F I B 1984 *Phys. Rev. Lett.* **53** 588

[14] Fisher D S, Halperin B I and Platzman P M 1979 *Phys. Rev. Lett.* **42** 798

[15] Guo C J, Mast D B, Mehrotra R, Ruan Y-Z, Stan M A and Dahm A J 1983 *Phys. Rev. Lett.* **51** 1461

[16] Kono K 1987 *J. Phys. Soc. Japan* **56** 1111